HHS Public Access

Author manuscript

Hepatology. Author manuscript; available in PMC 2020 December 01.

Published in final edited form as:

Hepatology. 2019 December ; 70(6): 2156–2170. doi:10.1002/hep.30772.

Rat OATP1A1 Interacts Directly With OATP1A4 Facilitating Its Maturation and Trafficking to the Hepatocyte Plasma Membrane

Pijun Wang[1], **Wen-Jun Wang**[1,2], **Jo Choi-Nurvitadhi**[1,2], **Yaniuska Lescaille**[1,3], **John W. Murray**[1,2], **Allan W. Wolkoff**[1,2,3]

[1]Marion Bessin Liver Research Center, Albert Einstein College of Medicine and Montefiore Medical Center, Bronx, New York 10461, USA

[2]Department of Anatomy and Structural Biology, Albert Einstein College of Medicine and Montefiore Medical Center, Bronx, New York 10461, USA

[3]Division of Hepatology, Albert Einstein College of Medicine and Montefiore Medical Center, Bronx, New York 10461, USA

Abstract

Organic anion transport proteins (OATPs) on the basolateral surface of hepatocytes mediate uptake of a number of drugs and endogenous compounds. Previous studies showed that rat OATP1A1 (rOATP1A1) has a PDZ consensus binding motif at its C-terminus and binds to PDZK1 which is required for its cell surface localization. PDZK1 associates with rOATP1A1-containing endocytic vesicles within cells, mediating recruitment of motor proteins required for microtubule-based trafficking to the plasma membrane. rOATP1A4 also traffics to the plasma membrane although it lacks a PDZ binding consensus sequence. The current study was designed to test the hypothesis that trafficking of rOATP1A4 to the plasma membrane requires its direct interaction with rOATP1A1 resulting in a complex that traffics through the cell in common subcellular vesicles in which the cytosolic tail of rOATP1A1 is bound to PDZK1. We found that 74% of rOATP1A4-containing rat liver endocytic vesicles (n=12,044) also contained rOATP1A1. Studies in transfected HEK293 cells showed surface localization of rOATP1A1 only when coexpressed with PDZK1 while rOATP1A4 required coexpression with rOATP1A1 and PDZK1. Studies in stably transfected HeLa cells that constitutively expressed PDZK1 showed that co-expression of rOATP1A4 with rOATP1A1 resulted in more rapid appearance of rOATP1A4 on the plasma membrane and faster maturation to its fully glycosylated form. Similar results were seen on immunofluorescence analysis of single cells. Immunoprecipitation of rat liver or transfected HeLa cell lysates with rOATP1A1 antibody specifically co-immunoprecipitated rOATP1A4 as determined by Western blot. *Conclusion:* These studies indicate that optimal rOATP1A4 trafficking to the cell surface is dependent upon co-expression and interaction with rOATP1A1. As rOATP1A1 binds to the chaperone protein PDZK1, rOATP1A4 functionally hitchhikes through the cell with this complex.

Contact Information for Corresponding Author: Allan W. Wolkoff, M.D., Marion Bessin Liver Research Center, 517 Ullmann Building, Albert Einstein College of Medicine, 1300 Morris Park Ave, Bronx, NY 10461, Tel: 718-430-3798, Fax: 718-430-8568, allan.wolkoff@einstein.yu.edu.

Keywords

transporter; PDZ; organic anion; endocytic vesicle; coexpression

Previous studies showed that the hepatocyte efficiently eliminates organic anions from the circulation with single pass extraction as high as 50% or greater (1). Pharmacokinetic studies were consistent with carrier-mediation (2, 3) and subsequent functional cloning experiments identified a transport protein, initially named organic anion transporting polypeptide (OATP) (4, 5). This 75 kDa glycoprotein has 12 transmembrane domains (6) and is sufficient to mediate ligand transport when transfected into various cell lines (7, 8). Since its initial discovery, over 20 additional members of the OATP family have been described (1). All are 12 transmembrane domain glycoproteins with overlapping substrate specificities and tissue distributions. The original OATP is now known as rOATP1A1 and is a member of the Solute Carrier Organic Anion Transporter (SLCO) family (9) with the gene name *Slco1a1*.

Our previous studies revealed that the C-terminal 4 amino acids of rat and mouse rOATP1A1 (KTKL) encode a PDZ consensus binding motif that binds to PDZK1 (10). This interaction with PDZK1 is required for efficient trafficking of rOATP1A1 to the basolateral plasma membrane of hepatocytes (10). Studies in PDZK1 knockout mice showed that surface localization of rOATP1A1, but not total cell content, was reduced as was uptake of BSP (10). Experiments performed in transfected cell lines confirmed that interaction with PDZK1 enhances cell surface expression of rOATP1A1 (11), suggesting trafficking between an intracellular endocytic vesicular pool and the cell surface (11). Further studies showed that these rOATP1A1-associated endocytic vesicles could bind to and move along microtubules (12, 13). *In vitro* motility studies of endocytic vesicles associated with rOATP1A1 and PDZK1 prepared from wild type mice showed selective recruitment of kinesin-1, a plus end directed motor molecule that traffics its cargo along microtubules towards the cell surface (12). Vesicles prepared from PDZK1 knockout mice are largely associated with dynein, a minus end directed motor molecule that traffics its cargo away from the cell surface (12).

Although many members of the OATP family possess PDZ consensus binding motifs at their C-termini, an almost equal number do not (1). In particular, rat rOATP1A4 does not have a PDZ binding motif while its very close mouse homolog does (KTKL). Despite lack of interaction with a PDZ protein, rat rOATP1A4 can still traffic to the basolateral plasma membrane of hepatocytes (14). We hypothesized that rOATP1A4 can interact with rOATP1A1 and traffic through the cell in common endocytic vesicles. This was examined in the present study.

Materials and Methods

Plasmids

pMEP4-rOATP1A4: rOATP1A4 cDNA cloned in the plasmid pCR2.1 was a gift from Dr. Richard Kim (University of Western Ontario, Canada) (15). The rOATP1A4 cDNA was recloned into pMEP4, a vector in which expression is under the zinc-inducible

metallothionein IIa promoter (7). In brief, rOATP1A4-PCR2.1 and pMEP4 were linearized with KpnI and BamHI respectively, and filled in to generate blunt ends. The resulting DNAs were digested with XhoI and the rOATP1A4 cDNA was ligated into the pMEP4 plasmid.

pCDNA3.1/Zeo (−)-mRFP-rOATP1A4: This plasmid encodes a monomeric red fluorescent protein (mRFP) fused to the N-terminus of rOATP1A4. rOATP1A4 cDNA was amplified by PCR from a previously described pCDNA3.1/Zeo(−)-rOATP1A4 plasmid (16) using as sense primer 5'-GGGCAGATGGAGGGAAAATGGGAAAATCTGAGAAAAG-3' and antisense primer 5'AACGGTACCAACTCAGTC CTC CGTCACTTT-3' that contains a KpnI restriction site. mRFP was amplified by PCR from a mRFP plasmid kindly provided by Dr. Erik Snapp (17) with a sense primer 5'-GTTCTCGAGGTTATGGTGTCCGAGCTGATTAAG-3' containing an XhoI restriction site and antisense primer 5'-CTTTTCTCAGATTTTCCCATTTTCCCTCCATCGCCTGCCC-3'. PCR products were purified using the QIAquick®PCR purification kit from Qiagen (Limburg, Netherlands). A 1:1 ratio of purified DNA product was allowed to run for 3 cycles of denaturation, annealing and extension before the addition of primers containing restriction sites KpnI and XhoI for another 25 cycles (18). The PCR ligated mRFP-rOATP1A4 was gel purified and subjected to another round of PCR amplification using the two restriction site containing primers. The final PCR product was inserted into the XhoI and KpnI restriction sites of pCDNA3.1/Zeo (−).

GFP-rOATP1A1: The superfolder GFP (sfGFP) plasmid was a kind gift of Dr. Erik Snapp. rOATP1A1 cDNA was prepared following digestion of a previously described mEGFP-rOATP1A1 plasmid (11) with Bgl II and XbaI and inserted into the sfGFP plasmid at these sites. A monomeric Enhanced GFP (mEGFP)-rOATP1A1 was prepared as described previously (11)

pFLAG-CMV-5c-PDZK1: This FLAG-tagged murine PDZK1 plasmid was prepared as described previously (16).

All plasmids were confirmed by full-length sequencing using appropriate primers in the Einstein sequencing facility.

Cell culture: HEK293 and HeLa cells were obtained from the Cell Culture and Genetic Engineering Core of the Marion Bessin Liver Research Center at Einstein which also validated their identities. Cells were grown in high glucose Dulbecco's Modified Eagle's growth medium (DMEM, Life Technologies, Inc.) supplemented with 10% fetal bovine serum (Bio-West, Midland, Texas), 100 units/ml penicillin and 0.1 mg/ml streptomycin (Life Technologies, Inc.).

Cell transfection: Transient transfection of plasmid constructs was performed in HEK293 cells with PolyFect Transfection Reagent (Qiagen, Limburg, Netherlands), using the manufacturer's conditions for HeLa cells. HeLa cell lines stably expressing rOATP1A1 under regulation of a zinc-inducible promoter were prepared by transfection of cells with pMEP4-rOATP1A1 as we described previously (7). Similar methods were used to prepare a pMEP4-rOATP1A4 HeLa cell line stably expressing rOATP1A4. To prepare a HeLa cell line

expressing both transporters, pMEP4-rOATP1A1 HeLa cells were transfected simultaneously with pMEP4-rOATP1A4 and pCDNA3.1/Neo using PolyFect. Stable transfectants were grown in the presence of hygromycin (200μg/ml) and neomycin G418 (1.2mg/ml) and were screened for rOATP1A1 and rOATP1A4 expression by Western blot analysis after incubation in 150 μM zinc sulfate for 48 hours.

Antibodies: Antibodies to C-terminal regions of rOATP1A1 and rOATP1A4 used for immunofluorescence and Western blot studies were prepared as described previously (16, 19). N-terminal antibody to rOATP1A1 was prepared similarly as described previously (16). Mouse monoclonal anti-FLAG antibody was obtained from Sigma (St, Louis, MO). Horseradish peroxidase-conjugated affinity-purified goat anti-rabbit IgG and goat anti-mouse IgG were obtained from GE healthcare Biosciences (Piscataway, NJ). Fluorescent secondary Cy5 affinity purified goat anti-rabbit IgG (product #111-175-144), Cy3 affinity purified goat anti-rabbit IgG (product #111-165-144), and Alexa Fluor 647 affinity purified goat anti-mouse IgG (product #115-605-166) were purchased from Jackson ImmunoResearch (West Grove, PA). Mouse monoclonal antibody to human PDZK1 (product #NBP2-22568) was obtained from Novus Biologicals (Littleton, CO).

Preparation and immunofluorescence labeling of endocytic vesicles from rat liver: Endocytic vesicles were prepared from rat liver as previously described (20). All procedures utilizing animals were approved by the Animal Use Committee of the Albert Einstein College of Medicine. Immunofluorescence labeling of vesicles was performed in optical chambers with a capacity of approximately 5 μl as we have described previously (12, 21). In some experiments co-association of rOATP1A1 and rOATP1A4 in vesicles was examined by immunofluorescence using antibodies that were prepared to each protein in rabbits. In these studies, endocytic vesicles were mixed in PMEE buffer (35 mM K_2-PIPES, 2 mg/ml BSA, 5 mM $MgCl_2$, 1 mM EGTA, 0.5 mM EDTA, 4 mM DTT and 2 mg/ml ascorbic acid, pH 7.4) and flowed into an uncoated optical chamber as previously described (22). Wash buffer (35 mM K_2-PIPES, 2 mg/ml BSA, 5 mM $MgCl_2$, 1 mM EGTA, 0.5 mM EDTA, 4 mM DTT, 5 mg/ml casein, pH 7.4) was used to dilute reagents and for washes. Vesicles in chambers were sequentially labeled with rabbit antibodies to rOATP1A4 and rOATP1A1 following the Multiple Immunofluorescent Labeling Protocol from the Multiple Antigen Labeling Guide from Vector Laboratories, which utilizes biotin labeled secondary antibodies and detection by fluorescent streptavidin. We followed blocking steps in the protocol including an incubation with high concentration unlabeled anti-rabbit antibody between primary antibody binding steps, according to the manufacturer's instructions. In brief, vesicles were washed two times and incubated for 2 min with StrepA block, from the streptavidin/biotin blocking kit (Vector Laboratories, #SP2002), diluted 1:10 in wash buffer. Subsequently, affinity purified rOATP1A4 antibody (1:200 dilution) was added to the chamber and incubated for 6 min. Vesicles were then washed four times and incubated for 6 min with biotinylated horse anti-rabbit IgG (H+L) (Vector Laboratories) at a1:250 dilution. After four additional washes, DyLight 647 streptavidin (Vector Laboratories) was added (1:300) to the chamber and incubated for 6 min, then washed two times. Vesicles were incubated for 6 min with unconjugated horse anti rabbit IgG (1:75) to block any unbound rabbit IgG. The StrepA block step was then repeated followed by a 2 min biotin block at

1:10 dilution to prevent interaction with the second streptavidin addition. These procedures were repeated for binding of primary rOATP1A1 antibody at a 1:1000 dilution and secondary antibody and DyLight 488 streptavidin. The stained vesicles were kept in PMEE buffer containing ascorbic acid without casein until microscopy was performed. Appropriate controls without one or both primary and/or secondary antibodies were performed to check for cross reaction during immunostaining.

Immunofluorescence studies in cells: HEK293 cells were transfected in 35 mm culture dishes, replated after 24 hours in 8 well Glass Chambers (Nunc Lab-Tek Chambered Coverglass #155411) at 70-80% confluence and grown in DMEM growth medium for an additional 24 hours. HeLa cells were seeded directly in these chambers and expression of rOATP1A1 or/and rOATP1A4 could be induced by addition of 150 μM $ZnSO_4$. Cells were fixed with 4% paraformaldehyde (Electron Microscopy Sciences, Hatfield, PA) in PBS for 15 min and permeabilized with 0.01% saponin in PBS for an additional 10 min at room temperature. Cells were washed three times with PBS for 3 min each and were blocked in 10% fetal bovine serum (FBS) in PBS for 30 min. They were then incubated in primary antibodies diluted in blocking buffer for 1 hour. Antibody was removed with two quick PBS washes and three additional 5 min washes. Appropriate fluorescent secondary antibodies diluted in blocking buffer was added and incubated for 1 hour. After two quick washes 10μM Hoechst 33342 (Sigma) nuclear dye was added to the cells for 15 min. After washing five times with PBS for 5 min per wash, stacked confocal images were taken at 60x magnification and merged using ImageJ and Photoshop.

Assay of cell surface expression of rOATP1A1 and rOATP1A4 in HeLa cell lines: 1-1.5×10^6 cells were plated in 60 mm dishes (Corning #430166) and induced for 4 or 24 hours with 150 μM $ZnSO_4$ in antibiotic free medium. Cells were then washed three times with ice-cold PBS/CM buffer (PBS containing 0.9 mM $CaCl_2$ and 0.33 mM $MgCl_2$) at pH 7.2, and were biotinylated at 4°C for 1 hour with 0.5 mg/ml of the membrane-impermeant biotinylation reagent sulfo-NHS-SS-biotin (Pierce) in PBS/CM, pH 8.0 as described previously (11). Cells were then washed once with ice-cold 50 mM Tris-HCl in PBS/CM, pH 8.0 and incubated on ice for 5 min to quench any unreacted reagent. After two additional washes with PBS, pH 7.4, cell pellets were harvested, frozen on dry ice, and lysed for 30 min at 4°C in 350 μl lysis buffer (PBS containing 1% Triton X-100, 1x protease inhibitor [Sigma# P8340], pH 7.4). Following centrifugation, supernatants were adjusted to a concentration of 350 μg protein/500 μl and were rotated overnight at 4°C with 50 μl of prewashed Streptavidin-agarose beads (Pierce). Beads were washed with 10 ml ice-cold lysis buffer, and biotinylated proteins were released by adding SDS sample buffer containing 0.1 M DTT and heating for 5-10 min at 95°C. These eluates and starting cell lysates were subjected to Western blot analysis for detection of rOATP1A1 or rOATP1A4.

Assay of the glycosylation state of rOATP1A1 and rOATP1A4 in HeLa cell lines: OATP-expressing HeLa cells that had been incubated for 4 or 24 hours in 150 μM $ZnSO_4$ were harvested in PBS containing 1% NP40, 1 mM EDTA, and protease inhibitors. Peptide N-Glycosidase F (PNGase F) and Endoglycosidase H (Endo H) were obtained from New England Biolabs, Inc (Ipswich, MA). Cell lysates were incubated with these enzymes

according to the manufacturer's directions except that denaturation was performed at room temperature for 10 min rather than at 100 °C. Lysates were then incubated with enzyme for 2 hr at 37 °C. Controls in which cell lysates were subjected to all procedures without enzyme addition were also performed. Changes in migration of OATPs due to deglycosylation were assessed by immunoblot.

Immunoprecipitation studies: HeLa cells expressing OATPs were washed with PBS, harvested from culture dishes, and pelleted at low speed (2000 rpm). Livers from DPPIV (−) male Fisher rats (23) obtained from the Einstein Liver Research Center Animal Models, Stem Cells and Cell Therapy Core were Dounce homogenized in PBS containing protease inhibitors and 1 mM EDTA pH7.4 and filtered through cheesecloth. Cells and liver homogenates were incubated for 60 min on ice in PBS containing 1% Chaps, 1mM EDTA, and protease inhibitors then centrifuged at 20,000 × g for 30 min at 4°C, and supernatants were incubated overnight at 4°C with non-immune rabbit IgG or affinity purified rOATP1A1 or rOATP1A4 antibody attached to protein A/G agarose beads (Santa Cruz Biotechnology, Dallas, TX) prepared as we described previously (16). Beads were washed with PBS containing 1% Chaps and 1mM EDTA, incubated with SDS-PAGE sample buffer containing 0.1M DTT, centrifuged, and the supernatant was subjected to Western blot analysis for detection of rOATP1A1.

Quantification of uptake of ^{35}S-BSP and ^{3}H-digoxin: ^{35}S-bromosulfophthalein (^{35}S-BSP) at a specific activity of 4800 μCi/μmol was synthesized as described previously (24). ^{3}H-digoxin (26.3Ci/mmol) was obtained from PerkinElmer (Shelton, CT). Uptake was quantified as described previously (7). Uptake data was fit, using SigmaPlot v11.2 (Systat Software, Inc., San Jose, CA), to the equation $v = \frac{Vmax[S]}{Km + [S]} + a[S]$ where v is the initial rate of uptake of ^{35}S-BSP, [S] is the concentration of ^{35}S-BSP, and a is a linear term representing non-carrier mediated diffusional uptake (25). Saturation kinetics of ^{35}S-BSP uptake by HEK293 cells expressing mEGFP-OATP1A1 was also determined. Time-dependent uptake of 0.1 μM ^{3}H-digoxin was assessed over 10-15 minutes using an identical protocol. As uptake of ^{3}H-digoxin was not seen (see below) saturation kinetics were not assayed. Cell protein was determined in replicate plates by the BCA assay (Pierce) according to the manufacturer's instructions with BSA as the standard.

Results

Co-localization and interaction of rOATP1A1 and rOATP1A4 in endocytic vesicles prepared from rat liver

rOATP1A1 and rOATP1A4 were colocalized in 74% of the 12,044 endocytic vesicles that were examined. (Figure 1A). The fact that they are colocalized in common vesicles does not imply that they are bound to each other. This was examined by immunoprecipitation of rat liver lysate with non-immune rabbit IgG or with rabbit antibodies to rOATP1A1 or rOATP1A4. Immunoprecipitates were analyzed by Western blot with antibody against rOATP1A1. We found that these immunoblots were optimal when run in the absence of reduction. As seen in the representative study in Figure 1B, antibody to rOATP1A4 immunoprecipitated rOATP1A1 (4th lane) while there was no reactivity when non-immune

IgG was used (2nd lane). rOATP1A1 immunoprecipitated itself as seen in the 3rd lane. We were unable to demonstrate rOATP1A4 in rOATP1A1 immunoprecipitates although it immunoprecipitated itself (data not shown).

Immunofluorescence studies in transfected HEK293 cells

When expression plasmids encoding sfGFP-rOATP1A1 or mRFP-rOATP1A4 were transfected individually into HEK293 cells, these transporters were distributed throughout the cell, without a clear surface membrane distribution (Figure 2A). With PDZK1 co-transfection, mRFP-rOATP1A4 was still distributed throughout the cell (Figure 2B, top panels) while sfGFP-rOATP1A1 was largely localized to the plasma membrane (Figure 2B, bottom panels). When sfGFP-rOATP1A1 and mRFP-rOATP1A4 were cotransfected into HEK293 cells in the absence of PDZK1, they were both distributed primarily throughout cells (Figure 2C, top panels). In contrast, both sfGFP-rOATP1A1 and mRFP-rOATP1A4 showed strong plasma membrane localization when co-transfected with PDZK1 (Figure 2c, bottom panels).

Immunoblot studies of OATP expression in transfected HeLa cell lines

Parental HeLa cells express PDZK1 endogenously (Figure 3, left panel). Studies were next performed in HeLa cells stably transfected with rOATP1A1, rOATP1A4, or both under control of a zinc-inducible promoter. There was no detectable expression of either transporter in cells grown in the absence of $ZnSO_4$ for 48 hours contrasting with transporter expression in cells cultured with $ZnSO_4$ (Figure 3). These results suggested that a pulse-chase type of study could be performed to look at early events in transporter trafficking. Transporter synthesis was initiated with the addition of zinc and trafficking of transporters to the cell surface was determined 4 and 24 hours later using a surface biotinylation and streptavidin pull down strategy. As seen in Figures 4 A and B, after 4 hours of zinc addition, the majority of immunodetectable rOATP1A1 and rOATP1A4 appeared at a lower molecular weight, indicated by the asterisks, as compared to their mature forms as seen in rat liver homogenate. These low molecular weight OATPs suggest altered glycosylation similar to the unglycosylated immature forms that we described previously (6, 19). Identification of surface proteins by Western blot following surface biotinylation and streptavidin-agarose pulldown, revealed only the fully mature forms of these proteins (arrowheads). The lower immunoblots on each panel are for GAPDH, an intracellular protein that is present in the cell lysate but is not labeled by biotin, validating that only proteins that reside on the cell surface are detected in the streptavidin pulldown. Antibody specificity was confirmed by including a lane of rat liver homogenate that had been extracted with 0.1 M Na_2CO_3 (RL Extract) as we have described previously (19). Soluble proteins such as GAPDH are removed by this carbonate extraction procedure and are not seen in these lanes. As seen in Panel A, rOATP1A1 that had trafficked to the cell surface (arrowhead) was seen in cells that had been singly transfected with rOATP1A1 as well as in cells that had been doubly transfected with rOATP1A1 and rOATP1A4. In contrast, at 4 hours of zinc addition, rOATP1A4 was expressed on the cell surface only when coexpressed with rOATP1A1 (arrowhead, panel B). By 24 hours after zinc addition, little lower molecular weight transporter is seen in any of the cell lines (Panels C and D). At this time, both rOATP1A1 and rOATP1A4 are found on the cell surface whether they are co-expressed or not.

To better characterize the immature forms of the transporters, cell lysates were incubated with the glycosidases PNGase F or Endo H. PNGase F removes all N-linked carbohydrate from glycoproteins, while Endo H removes only high mannose forms that are typically located in the endoplasmic reticulum (ER) during protein biosynthesis (26, 27). PNGase F incubation resulted in removal of N-linked carbohydrate chains (deglycos) from both the mature and immature forms of rOATP1A1 and rOATP1A4 as seen by reduced molecular weight on immunoblot (Figure 5A). This implies that the immature form of these proteins, seen at 4 hours following induction of synthesis by addition of zinc, still contain N-linked carbohydrate. These immature proteins are deglycosylated following incubation with Endo H while the mature forms are not (Figure 5B). These data indicate that the immature transporters contain high mannose carbohydrate chains and are most likely located in the ER, prior to final processing in the Golgi.

We also asked whether rOATP1A1 and rOATP1A4 interact with each other when coexpressed in the HeLa cell line. rOATP1A1 was not immunoprecipitated from doubly transfected, rOATP1A1/rOATP1A4, HeLa cell lysate with non-immune IgG (Figure 5C). When antibody to rOATP1A1 was used, the major band in the immunoprecipitate following a 4 hour exposure of cells to zinc corresponded to its immature form (open arrowhead) with a less intense band corresponding to its mature fully processed form (black arrowhead). This latter band became the dominant band in the immunoprecipitate from cells following a 24 hour exposure to zinc. When immunoprecipitation was performed with antibody to rOATP1A4, both immature and mature forms of rOATP1A1 were recovered in the immunoprecipitates. This is consistent with their direct interaction during early biosynthesis in the ER, before the final glycosylation processing in the Golgi. We were unable to demonstrate rOATP1A4 in rOATP1A1 immunoprecipitates at either time point (data not shown).

Immunofluorescence studies of OATP expression in transfected HeLa cell lines

The studies presented above provide information regarding OATP biosynthesis in the entire population of HeLa cells. We next studied subcellular distribution profiles in single cells by immunofluorescence microscopy. As seen in Figure 6, 4 hours following zinc addition, some rOATP1A1 was distributed as punctae on the cell surface whether or not it was coexpressed with rOATP1A4 (left panels, short arrows). In contrast, rOATP1A4 expression at 4 hours was predominantly intracellular (long arrows) when expressed alone but when coexpressed with rOATP1A1 punctate surface expression was seen. At 24 hours, rOATP1A1 was expressed continuously along the plasma membrane (arrowheads) whether expressed alone or together with rOATP1A4. Distribution of rOATP1A4 at 24 hours was punctate on the cell surface when expressed alone and continuous on the cell surface when expressed together with rOATP1A1.

Uptake kinetics of ^{35}S-BSP by transfected HeLa cell lines and HEK293 cells

Uptake of ^{35}S-BSP by HeLa cells expressing rOATP1A1 alone or together with rOATP1A4 was determined as in Methods. Although there was a substantial increase in V_{max} between 4 and 24 hours of incubation of cells in zinc, there was no significant difference in parameters in cells expressing only rOATP1A1 vs those coexpressing rOATP1A1 and rOATP1A4 (Table

1). There was little difference in uptake by either group of cells at 4 hr of zinc addition as compared to uninduced cells. Representative uptake curves are presented in Supplemental Figure 1. Uptake of ^{35}S-BSP by HEK293 cells expressing mEGFP-rOATP1A1 was also saturable indicating that the GFP-associated transporter retained its transport activity (supplemental Figure 2). Although previous studies indicated that rOATP1A4 could mediate uptake of digoxin (28), we were unable to demonstrate uptake of ^{3}H-digoxin by rOATP1A4 expressing HeLa cells whether expressed alone or together with rOATP1A1 (Supplemental Figure 3).

Discussion

The members of the organic anion transport protein (OATP) family that are expressed in the liver play an important role in uptake and metabolism of a variety of endogenous compounds and xenobiotics (9, 29). These proteins are localized to the basolateral (sinusoidal) plasma membrane of hepatocytes and also have a substantial intrahepatic pool in endocytic vesicles (12). In previous studies, we found that rat and mouse OATP1A1 has a PDZ consensus sequence (KTKL) at the C-terminus that binds to PDZ domains 1 and 3 of PDZK1 (16). In mice in which PDZK1 has been knocked out, trafficking of OATP1A1 to the plasma membrane is reduced (10-12) resulting in decreased transport activity due to accumulation of the transporter in endocytic vesicles within hepatocytes (10). In contrast to rOATP1A1, rOATP1A4 lacks a PDZ consensus binding site but still traffics to the plasma membrane of hepatocytes. Interestingly, mouse OATP1A4 which is highly homologous to the rat protein, has the KTKL PDZK1 binding consensus sequence at its C-terminus. We hypothesized that rOATP1A1 and rOATP1A4 traffic together within rat hepatocytes where rOATP1A4 acts as a “hitchhiker” utilizing the rOATP1A1-PDZK1 trafficking mechanism. The results in this study are highly supportive of this notion.

Our previous studies showed that hepatocyte basolateral organic anion transporters including OATP1A1 and NTCP have substantial intracellular pools in endocytic vesicles that can traffic on microtubules towards and away from the cell surface using specific microtubule based molecular motors (12, 30). Our current studies indicate that rOATP1A4 is also associated with these vesicles (Figure 1A) where it is likely that it interacts directly with rOATP1A1 (Figure 1B). Amino acid sequence comparison of the OATP family reveals enrichment in cysteine with rOATP1A1 and rOATP1A4 sharing 25 conserved cysteines (31). Although it is possible that these transporters may interact via formation of disulfide bonds, their migration in Western blots in the absence of reduction did not differ from that in the presence of reduction (19), making this possibility unlikely. Whatever the mechanism, interaction of rOATP1A4 with rOATP1A1 is necessary for its PDZK1-dependent trafficking to the cell surface, as seen in studies performed in HEK293 cells (Figure 2). Studies in the HeLa cell lines that have endogenous expression of PDZK1 indicate that this interaction is an early event in transporter biosynthesis. Transporter expression in these cells is under regulation of a zinc-inducible promoter, and as there is essentially no transporter expression until zinc is added to the medium, a wave of de novo synthesized transporter can be followed. Trafficking of these proteins through the cell during biosynthesis can be assessed by their glycosylation state, as the OATPs are glycoproteins containing N-linked carbohydrate chains that are completed in the Golgi after protein synthesis in the ER (6). At

4 hours of zinc induction, the majority of each of the transporters was immunodetected in a low molecular weight form (Figure 4). These low molecular weight forms have N-linked carbohydrate that is removed by PNGase F (Figure 5A) as well as by Endo H (Figure 5B), indicating high mannose N-linked carbohydrate, consistent with localization in the ER (27). Interestingly, the low molecular weight form of rOATP1A1 was seen following immunoprecipitation of rOATP1A4 (Figure 5C), indicating that their association is initiated in the ER. Only the fully glycosylated forms of these transporters are found on the cell surface, as determined by a surface biotinylation procedure. At 4 hours of zinc addition, there was little rOATP1A4 on the cell surface unless it was co-expressed with rOATP1A1 (Figure 4B), suggesting that they traffic through the cell together. In contrast, at 24 hours of zinc addition, this facilitation of trafficking was not seen and rOATP1A4 was detected on the cell surface even in the absence of co-expression of rOATP1A1 (Figure 4D). However, although rOATP1A4 was detectable on the cell surface at 24 hours, its distribution in the absence of co-expression with rOATP1A1 was punctate along the cell surface as compared to a smooth surface distribution when co-expressed with rOATP1A1 (Figure 6). Of potential significance is the fact that rOATP1A1 has a similar punctate distribution on the cell surface at 4 hours after zinc addition and these cells transport ^{35}S-BSP poorly (Table 1). It is possible that interaction with other proteins on the cell surface is required for a more uniform distribution and fully optimal transporter activity. That these other proteins may be recruited by interaction with PDZK1 can be hypothesized. Previous studies showed that PDZK1 has 4 independent binding domains (PDZ 1-4) and that rOATP1A1 can bind to domains 1 and 3, leaving 2 and 4 potentially available to bind other ligands (16). In addition, PDZK1 also has a PDZ consensus sequence at its C-terminus that can interact with a PDZ binding domain on EBP50, another PDZ protein (32), thus establishing the potential for building a large scaffold of proteins associated with rOATP1A1, although further studies will be needed to clarify this.

These studies indicate that optimal rOATP1A4 trafficking to the cell surface is dependent upon co-expression and interaction with rOATP1A1. As rOATP1A1 binds to the chaperone protein PDZK1, rOATP1A4 functionally hitchhikes through the cell with this complex. There did not appear to be an effect of this transporter interaction on the ability of rOATP1A1 to transport ^{35}S-BSP, although it must be recognized that the stoichiometry of the two transporters in this HeLa cell system is unknown, and it is possible that the majority of rOATP1A1 is not bound to rOATP1A4. We have been unable to perform the corresponding transport study for rOATP1A4 as in our hands, BSP is not transported by rOATP1A4-expressing HeLa cells (data not shown) and other than sulfolithocholyltaurine (14), which is not readily available, we are unaware of specific ligands for this transporter. Digoxin has been shown to be taken up by hepatocytes (33) and rOATP1A4 has been the presumed transporter for this process based largely on data showing modest uptake of digoxin by rOATP1A4-cRNA injected Xenopus oocytes (28, 34). However, we have been unable to show uptake of digoxin in the rOATP1A4-inducible HeLa cell line (Supplemental Figure 3) and digoxin did not inhibit rOATP1A4-mediated uptake of sulfolithocholyltaurine by these cells (14). Uptake of digoxin by rOATP1A4 knockout mouse hepatocytes did not differ from wild type (35) while another pharmacokinetic study showed a subtle reduction in parameters of liver uptake of digoxin (36). Although there is some question about the

identity of rOATP1A4-specific substrates, we speculate that enhanced processing and targeting of rOATP1A4 to the cell surface via its interaction with rOATP1A1 should be an important determinant of its transport function.

We suggest that this hitchhiking paradigm will hold for other OATPs, especially those that are expressed in human liver. hOATP2B1 and hOATP1A2, both found in liver, bind to PDZK1 and this regulates their subcellular trafficking and function (37, 38). Although the C-terminal PDZ binding consensus sequence of hOATP1A2 (KTKL) is identical to that of rOATP1A1, hOATP2B1, terminates in the sequence DSRV, but is still a ligand for PDZK1. hOATP1B1, another transporter in human liver, has a C-terminal sequence (ETHC) which is predicted to bind to the first PDZ binding domain of PDZK1 (http://pow.baderlab.org) (39), while hOATP1B3 has a C-terminal sequence (AAAN) which is predicted not to bind to PDZK1 or other PDZ proteins. Of potential importance, data has been published suggesting that hOATP1B1 and hOATP1B3 may interact with each other when co-transfected into HEK293 cells (40). Although studies of the trafficking of these human OATPs is beyond the scope of the present study, the paradigms developed in this study will facilitate future elucidation of OATP interactions, trafficking, and function in human liver.

Supplementary Material

Refer to Web version on PubMed Central for supplementary material.

Acknowledgments

Financial Support:

This work was supported by the National Institutes of Health National Institute of Diabetes and Digestive and Kidney Diseases Grants DK23026, DK098408, and DK41296.

List of Abbreviations:

OATP	organic anion transport protein
PDZ	postsynaptic density protein, drosophila disc large tumor suppressor, zonula occludens-1 protein
PDZK1	PDZ domain containing 1
BSP	bromosulfophthalein
mRFP	monomeric red fluorescent protein
sfGFP	superfolder green fluorescent protein
KLH	keyhole limpet hemocyanin
PMEE buffer	35 mM K_2-PIPES, 2 mg/ml BSA, 5 mM $MgCl_2$, 1 mM EGTA, 0.5 mM EDTA, 4 mM DTT and 2 mg/ml ascorbic acid, pH 7.4

Wash buffer	35 mM K_2-PIPES, 2 mg/ml BSA, 5 mM $MgCl_2$, 1 mM EGTA, 0.5 mM EDTA, 4 mM DTT, 5 mg/ml casein, pH 7.4
PBS	phosphate buffered saline
PBS/CM buffer	PBS containing 0.9 mM $CaCl_2$, 0.33 mM $MgCl_2$, pH 7.2
TBS	150 mM NaCl, 50 mM Tris, 1 mM EDTA, pH7.4
SFM	serum free medium (135 mM NaCl, 1.2 mM $MgCl_2$, 0.81 mM $MgSO_4$, 27.8 mM glucose, 2.5 mM $CaCl_2$, 25 mM HEPES, pH 7.2)
BSA	bovine serum albumin
BCA	bicinchoninic acid

References:

1. Wolkoff AW. Organic anion uptake by hepatocytes. Compr. Physiol 2014;4:1715–1735. [PubMed: 25428858]
2. Scharschmidt BF, Waggoner JG, Berk PD. Hepatic organic anion uptake in the rat. J. Clin. Invest 1975;56:1280–1292. [PubMed: 1184749]
3. Min AD, Johansen KJ, Campbell CG, Wolkoff AW. Role of chloride and intracellular pH on the activity of the rat hepatocyte organic anion transporter. J. Clin. Invest 1991;87:1496–1502. [PubMed: 2022722]
4. Jacquemin E, Hagenbuch B, Stieger B, Wolkoff AW, Meier PJ. Expression of the hepatocellular chloride-dependent sulfobromophthalein uptake system in Xenopus laevis oocytes. J. Clin. Invest 1991;88:2146–2149. [PubMed: 1752967]
5. Jacquemin E, Hagenbuch B, Stieger B, Wolkoff AW, Meier PJ. Expression cloning of a rat liver Na(+)-independent organic anion transporter. Proc. Natl. Acad. Sci. U. S. A 1994;91:133–137. [PubMed: 8278353]
6. Wang P, Hata S, Xiao Y, Murray JW, Wolkoff AW. Topological assessment of oatp1a1: a 12 transmembrane domain integral membrane protein with three N-linked carbohydrate chains. Am J Physiol Gastrointest Liver Physiol 2008.
7. Shi X, Bai S, Ford AC, Burk RD, Jacquemin E, Hagenbuch B, Meier PJ, et al. Stable inducible expression of a functional rat liver organic anion transport protein in HeLa Cells. J. Biol. Chem 1995;270:25591–25595. [PubMed: 7592731]
8. Kanai N, Lu R, Bao Y, Wolkoff AW, Schuster VL. Transient expression of oatp organic anion transporter in mammalian cells: identification of candidate substrates. Am. J. Physiol 1996;270:F319–F325. [PubMed: 8779893]
9. Hagenbuch B, Stieger B. The SLCO (former SLC21) superfamily of transporters. Mol. Aspects Med 2013;34:396–412. [PubMed: 23506880]
10. Wang P, Wang JJ, Xiao Y, Murray JW, Novikoff PM, Angeletti RH, Orr GA, et al. Interaction with PDZK1 is required for expression of organic anion transporting protein 1A1 (OATP1A1) on the hepatocyte surface. J. Biol. Chem 2005;280:30143–30149. [PubMed: 15994332]
11. Choi JH, Murray JW, Wolkoff AW. PDZK1 binding and serine phosphorylation regulate subcellular trafficking of organic anion transport protein 1a1. Am. J. Physiol Gastrointest Liver Physiol 2011;300:G384–G393. [PubMed: 21183661]
12. Wang WJ, Murray JW, Wolkoff AW. Oatp1a1 requires PDZK1 to traffic to the plasma membrane by selective recruitment of microtubule-based motor proteins. Drug Metab Dispos 2014;42:62–69. [PubMed: 24115750]

13. Novikoff PM, Cammer M, Tao L, Oda H, Stockert RJ, Wolkoff AW, Satir P. Three-dimensional organization of rat hepatocyte cytoskeleton: relation to the asialoglycoprotein endocytosis pathway. J. Cell Sci 1996;109 (Pt 1):21–32. [PubMed: 8834787]
14. Meng LJ, Wang P, Wolkoff AW, Kim RB, Tirona RG, Hofmann AF, Pang KS. Transport of the sulfated, amidated bile acid, sulfolithocholyltaurine, into rat hepatocytes is mediated by Oatp1 and Oatp2. Hepatology 2002;35:1031–1040. [PubMed: 11981753]
15. Cvetkovic M, Leake B, Fromm MF, Wilkinson GR, Kim RB. OATP and P-glycoprotein transporters mediate the cellular uptake and excretion of fexofenadine. Drug Metab Dispos 1999;27:866–871. [PubMed: 10421612]
16. Wang P, Wang JJ, Xiao Y, Murray JW, Novikoff PM, Angeletti RH, Orr GA, et al. Interaction with PDZK1 is required for expression of organic anion transporting protein 1A1 on the hepatocyte surface. J Biol Chem 2005;280:30143–30149. [PubMed: 15994332]
17. Costantini LM, Fossati M, Francolini M, Snapp EL. Assessing the tendency of fluorescent proteins to oligomerize under physiologic conditions. Traffic 2012;13:643–649. [PubMed: 22289035]
18. An Y, Wu W, Lv A. A PCR-after-ligation method for cloning of multiple DNA inserts. Anal Biochem 2010;402:203–205. [PubMed: 20363207]
19. Bergwerk AJ, Shi X, Ford AC, Kanai N, Jacquemin E, Burk RD, Bai S, et al. Immunologic distribution of an organic anion transport protein in rat liver and kidney. Am. J. Physiol 1996;271:G231–G238. [PubMed: 8770038]
20. Murray JW, Bananis E, Wolkoff AW. Reconstitution of ATP-dependent movement of endocytic vesicles along microtubules in vitro: an oscillatory bidirectional process. Mol. Biol. Cell 2000;11:419–433. [PubMed: 10679004]
21. Murray JW, Bananis E, Wolkoff AW. Immunofluorescence microchamber technique for characterizing isolated organelles. Anal. Biochem 2002.
22. Bananis E, Murray JW, Stockert RJ, Satir P, Wolkoff AW. Microtubule and motor-dependent endocytic vesicle sorting in vitro. J Cell Biol 2000;151:179–186. [PubMed: 11018063]
23. Thompson NL, Hixson DC, Callanan H, Panzica M, Flanagan D, Faris RA, Hong WJ, et al. A Fischer rat substrain deficient in dipeptidyl peptidase IV activity makes normal steady-state RNA levels and an altered protein. Use as a liver-cell transplantation model. Biochem J 1991;273 (Pt 3): 497–502. [PubMed: 1705112]
24. Kurisu H, Nilprabhassorn P, Wolkoff AW. Preparation of [35S]sulfobromophthalein of high specific activity. Anal. Biochem 1989;179:72–74. [PubMed: 2757201]
25. Hata S, Wang P, Eftychiou N, Ananthanarayanan M, Batta A, Salen G, Pang KS, et al. Substrate specificities of rat oatp1 and ntcp: implications for hepatic organic anion uptake. Am. J. Physiol Gastrointest. Liver Physiol 2003;285:G829–G839. [PubMed: 12842829]
26. Maley F, Trimble RB, Tarentino AL, Plummer TH Jr. Characterization of glycoproteins and their associated oligosaccharides through the use of endoglycosidases. Anal Biochem 1989;180:195–204. [PubMed: 2510544]
27. Iavarone C, Ramsauer K, Kubarenko AV, Debasitis JC, Leykin I, Weber AN, Siggs OM, et al. A point mutation in the amino terminus of TLR7 abolishes signaling without affecting ligand binding. J Immunol 2011;186:4213–4222. [PubMed: 21383246]
28. Noé B, Hagenbuch B, Stieger B, Meier PJ. Isolation of a multispecific organic anion and cardiac glycoside transporter from rat brain. Proc. Natl. Acad. Sci. USA 1997;94:10346–10350. [PubMed: 9294213]
29. Wolkoff AW: Mechanisms of hepatocyte organic anion transport In: Johnson LR, Ghishan FK, Kaunitz JD, Merchant JL, Said HM, Wood JD, eds. Physiology of the Gastrointestinal Tract. Fifth Edition ed. San Diego: Academic Press, 2012; 1485–1506.
30. Wang X, Wang P, Wang W, Murray JW, Wolkoff AW. The Na(+)-Taurocholate Cotransporting Polypeptide Traffics with the Epidermal Growth Factor Receptor. Traffic 2016;17:230–244. [PubMed: 26650232]
31. Wolkoff AW: Mechanisms of Hepatocyte Organic Anion Transport In: Said HM, ed. Physiology of the Gastrointestinal Tract. Sixth Edition ed. San Diego: Academic Press, 2018; 957–979.
32. Lalonde D, Bretscher A. The scaffold protein PDZK1 undergoes a head-to-tail intramolecular association that negatively regulates its interaction with EBP50. Biochemistry 2009.

33. Liu L, Mak E, Tirona RG, Tan E, Novikoff PM, Wang P, Wolkoff AW, et al. Vascular binding, blood flow, transporter, and enzyme interactions on the processing of digoxin in rat liver. J Pharmacol Exp Ther 2005;315:433–448. [PubMed: 15994370]

34. Guo GL, Klaassen CD. Protein kinase C suppresses rat organic anion transporting polypeptide 1- and 2-mediated uptake. J. Pharmacol. Exp. Ther 2001;299:551–557. [PubMed: 11602666]

35. Gong L, Aranibar N, Han YH, Zhang Y, Lecureux L, Bhaskaran V, Khandelwal P, et al. Characterization of organic anion-transporting polypeptide (Oatp) 1a1 and 1a4 null mice reveals altered transport function and urinary metabolomic profiles. Toxicol. Sci 2011;122:587–597. [PubMed: 21561886]

36. Takano J, Maeda K, Kusuhara H, Sugiyama Y. Organic Anion Transporting Polypeptide 1a4 is Responsible for the Hepatic Uptake of Cardiac Glycosides in Mice. Drug Metab Dispos 2018;46:652–657. [PubMed: 29348124]

37. Zheng J, Chan T, Cheung FS, Zhu L, Murray M, Zhou F. PDZK1 and NHERF1 regulate the function of human organic anion transporting polypeptide 1A2 (OATP1A2) by modulating its subcellular trafficking and stability. PLoS. One 2014;9:e94712. [PubMed: 24728453]

38. Ferreira C, Hagen P, Stern M, Hussner J, Zimmermann U, Grube M, Meyer Zu Schwabedissen HE. The scaffold protein PDZK1 modulates expression and function of the organic anion transporting polypeptide 2B1. Eur J Pharm Sci 2018;120:181–190. [PubMed: 29752999]

39. Hui S, Xing X, Bader GD. Predicting PDZ domain mediated protein interactions from structure. BMC Bioinformatics 2013;14:27. [PubMed: 23336252]

40. Zhang Y, Boxberger KH, Hagenbuch B. Organic anion transporting polypeptide 1B3 can form homo- and hetero-oligomers. PLoS One 2017;12:e0180257. [PubMed: 28644885]

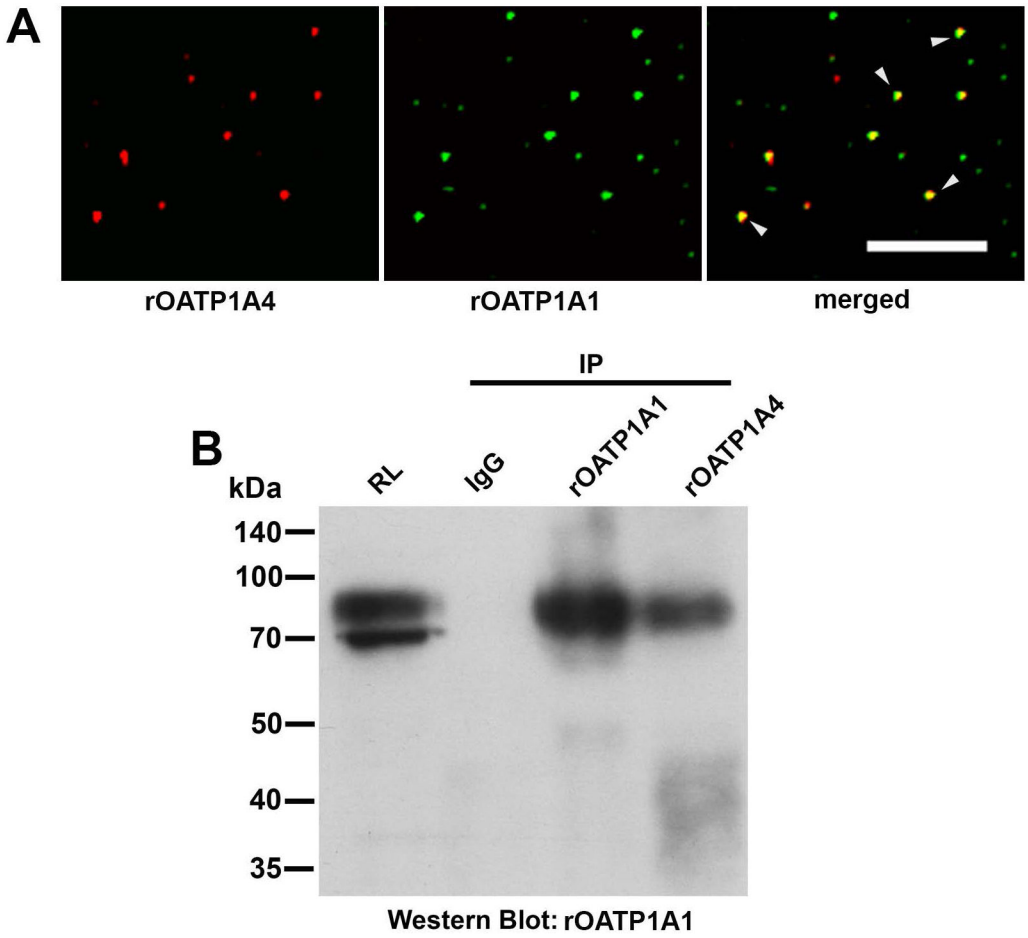

Figure 1: Interaction of rOATP1A1 and rOATP1A4 in rat liver.

A. Endocytic vesicles isolated from rat liver were immunostained for rOATP1A1 and rOATP1A4 using the two primary antibody method. Images from a representative study are shown in which rOATP1A4 is in red, rOATP1A1 is in green, and vesicles in which rOATP1A4 and rOATP1A1 are colocalized are in yellow (arrowheads) in the merged view. rOATP1A1 and rOATP1A4 were colocalized in 74% of the 12,044 vesicles that were examined. Scale bar = 10 μm. B. Colocalization in vesicles does not imply that rOATP1A1 and rOATP1A4 are bound to each other. This was examined by immunoprecipitation. Rat liver homogenate was prepared as in Materials and Methods, solubilized in 1% CHAPS containing protease inhibitors, and subjected to immunoprecipitation with non-immune IgG or antibody to rOATP1A1 or rOATP1A4. The immunoprecipitates were subjected to Western blot with antibody to rOATP1A1 in the absence of reduction. The starting rat liver lysate (RL) in CHAPS was used to show antibody reactivity and specificity.

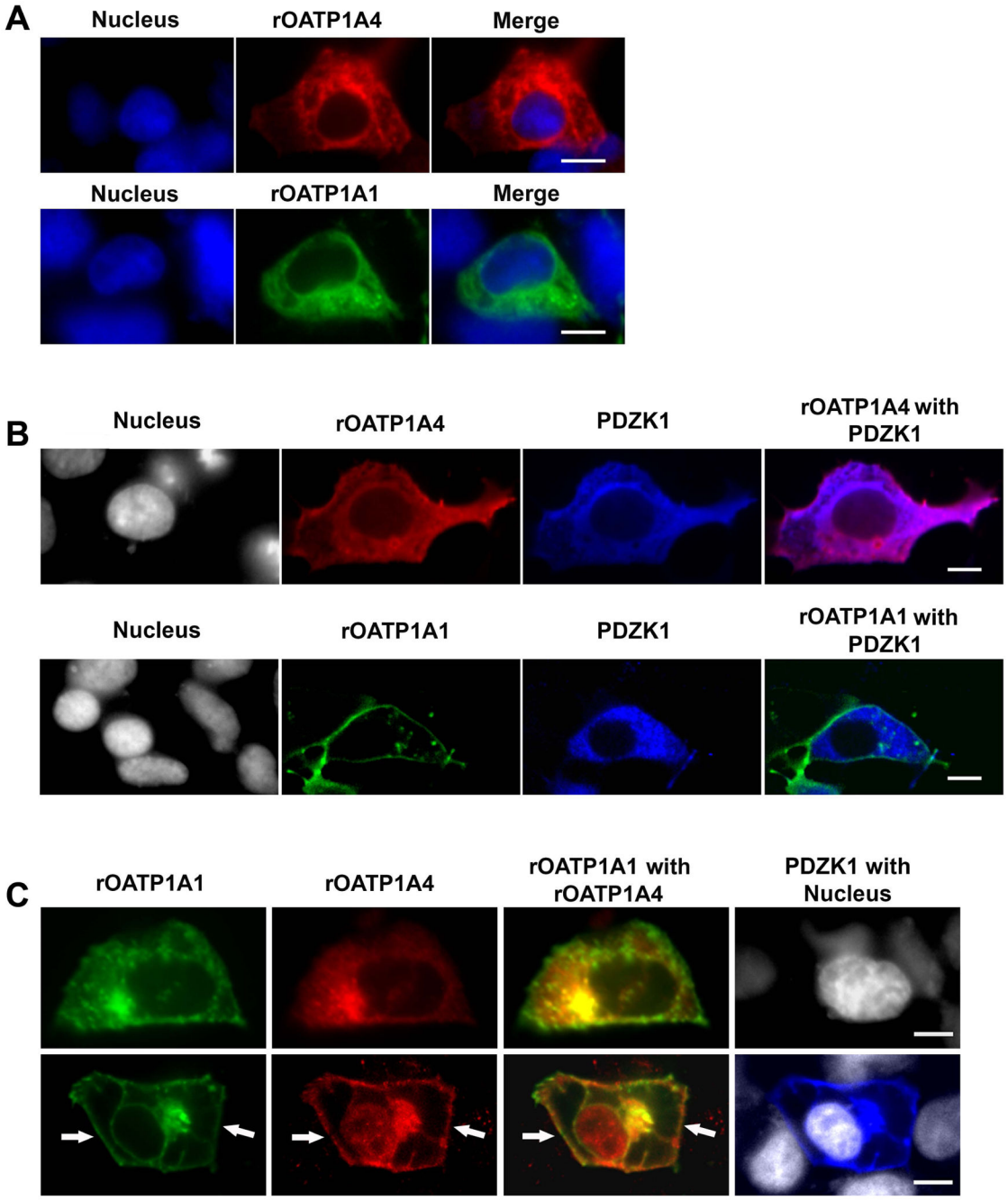

Figure 2: Subcellular localization of rOATP1A1 and rOATP1A4 when expressed singly and together in the presence or absence of PDZK1.

A. Human embryonic kidney (HEK) 293 cells were transfected with plasmid encoding sfGFP-rOATP1A1 or mRFP-rOATP1A4. Two days after transfection cells were fixed and stained with primary rOATP1A4 antibody followed by Cy5 secondary antibody and imaged by confocal microscopy with a 60x objective. Expression of sfGFP-rOATP1A1 is in green, mRFP-rOATP1A4 in red, and Hoechst 33342 stained nuclei in blue. **Top:** Representative images of mRFP-rOATP1A4 transfected HEK293 cells. **Bottom:** Representative images of sfGFP-rOATP1A1 transfected HEK293 cells. Both proteins are largely intracellular. Scale

bars = 10μm. **B.** HEK 293 cells expressing sfGFP-rOATP1A1 or mRFP-rOATP1A4 were transfected with pFLAG-PDZK1. Cells were fixed and labeled with rOATP1A4 and PDZK1 antibodies. Expression of sfGFP-rOATP1A1 is in green, mRFP-rOATP1A4 in red, PDZK1 in blue, and Hoechst 33342 stained nuclei in gray. Images were taken by confocal microcopy with a 60x objective. **Top:** Representative images of mRFP-rOATP1A4 and PDZK1 transfected HEK293 cells **Bottom:** Representative image of sfGFP-rOATP1A1 double transfected with PDZK1 in HEK293 cells. rOATP1A1 but not rOATP1A4 was distributed on the plasma membrane in the presence of PDZK1. Scale bars = 10μm. **C.** HEK 293 cells were transfected with plasmid encoding sfGFP-rOATP1A1, mRFP-rOATP1A4, and/or pFLAG-PDZK1. Cells were fixed and immunofluorescence labeled with rOATP1A4 and PDZK1 antibodies. Expression of sfGFP-rOATP1A1 is in green, mRFP-rOATP1A4 in red, PDZK1 in blue and Hoechst 33342 stained nuclei in gray. Images were taken by confocal microcopy with a 60x objective. **Top:** Representative images of mRFP-rOATP1A4 and sfGFP-rOATP1A1 double transfection in HEK293 cells. **Bottom:** Representative image of triple transfection with mRFP-rOATP1A4, sfGFP-rOATP1A1 and pFLAG-PDZK1 in HEK293 cells. White arrows point to plasma localization of the proteins. Scale bars = 10μm.

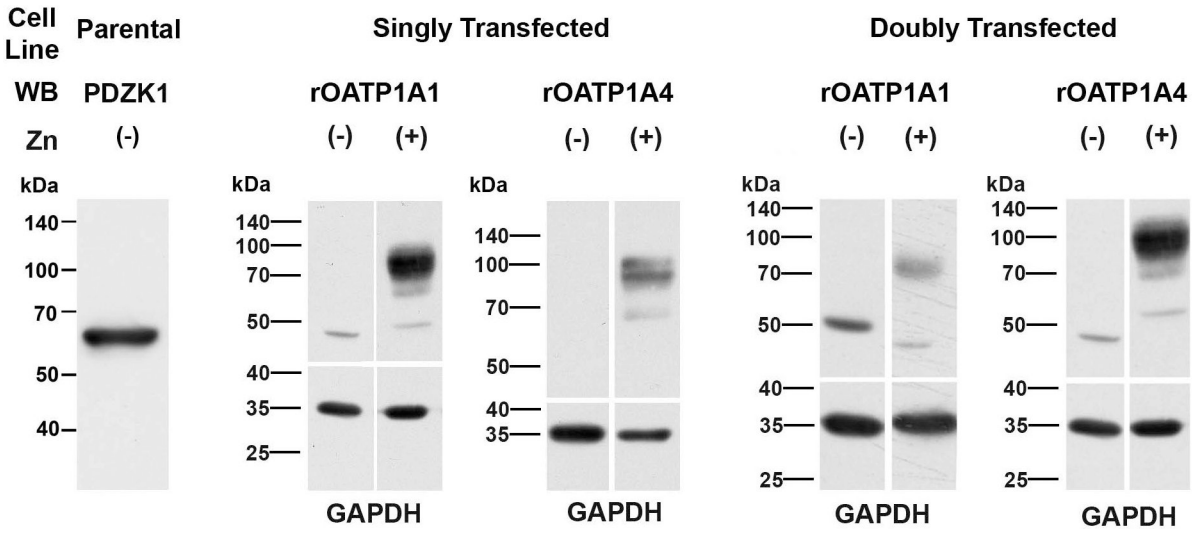

Figure 3: Expression of oatps in stably transfected HeLa cells is tightly regulated by zinc.

A 1% Triton X-100 lysate of untreated parental HeLa cells was subjected to Western blot (50 μg) to determine if there was endogenous expression of PDZK1 (leftmost lane). The other Western blots in this figure were performed on 1% Triton X-100 lysates of stably transfected HeLa cell lines expressing rOATP1A1 or rOATP1A4 (singly transfected) or both (doubly transfected) under regulation by a metallothionein promoter. These cell lines were prepared as in Materials and Methods and were incubated for 48 hours with or without 150 μM zinc added to the culture medium. OATP expression was examined by immunoblot as indicated in the figure. The lower panels show GAPDH expression, as a loading control.

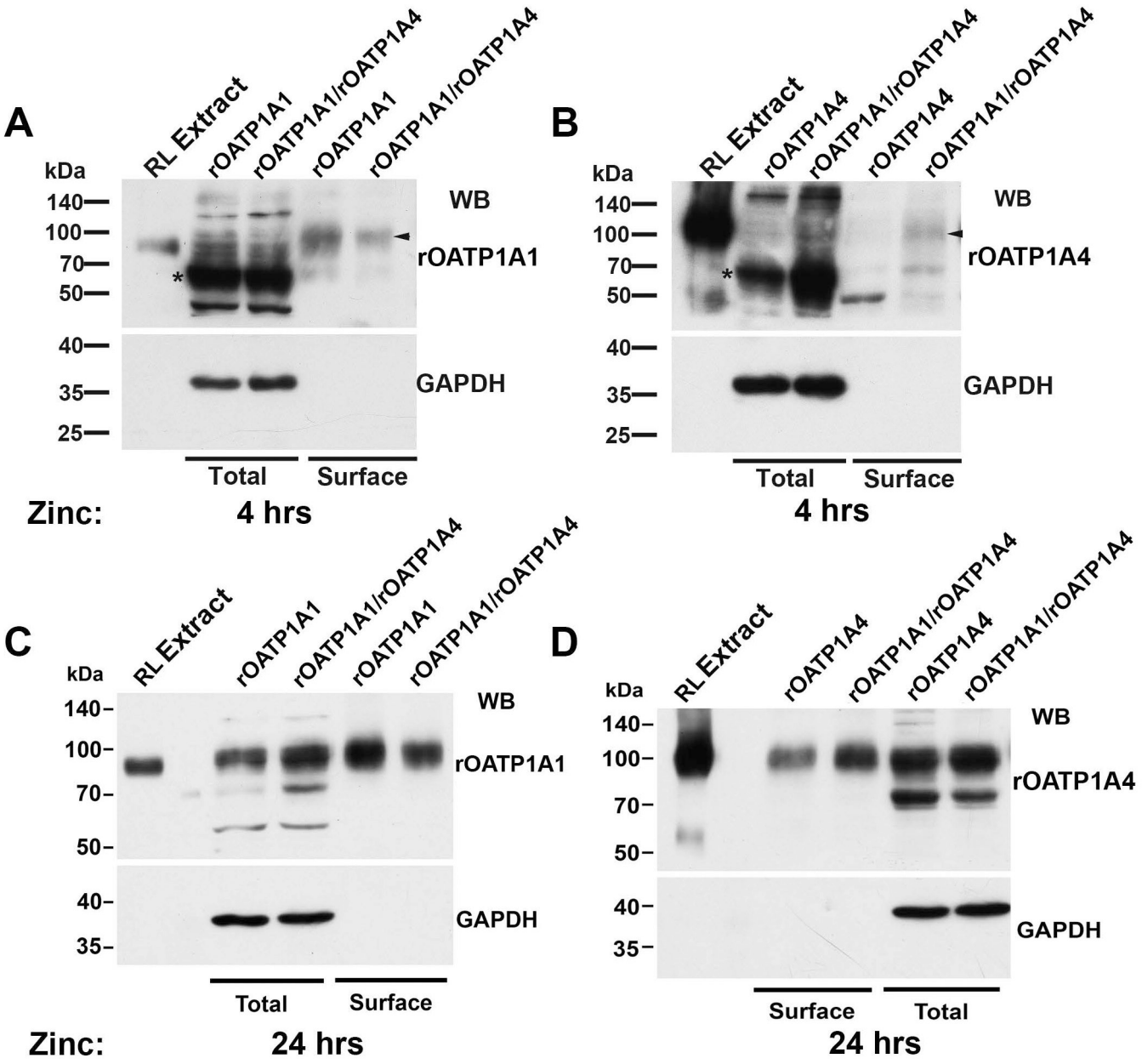

Figure 4: Coexpression of rOATP1A1 and rOATP1A4 facilitates trafficking of rOATP1A4 to the plasma membrane of stably transfected HeLa cells.

HeLa cell lines expressing rOATP1A1, rOATP1A4, or both under a metallothionein promoter were prepared and incubated for 4 or 24 hours, as indicated, in the presence of 150 μM zinc to initiate transporter expression. These cells endogenously express PDZK1. In all immunoblots in this figure, antibody specificity was confirmed by including a lane of rat liver homogenate that had been extracted with 0.1 M Na_2CO_3 (RL Extract) as we have described previously (19). Soluble proteins such as GAPDH are removed by this procedure and are not seen in these lanes. **Panels A-D:** Following zinc incubation, cells were surface biotinylated with a membrane impermeant reagent and lysed. An aliquot of lysate was processed for immunoblot (total) while the remainder was incubated with streptavidin

agarose to capture surface proteins. Surface expression of OATPs was assessed in these fractions by immunoblot. The lower panels show immunoblots for GAPDH, an intracellular protein that is present in the cell lysate but is not labeled by biotin, validating that only proteins that reside on the cell surface are detected in the streptavidin pulldown. The asterisks in Panels A and B indicate lower molecular weight forms of the transporters, consistent with incomplete glycosylation, and the arrowheads indicate mature fully glycosylated forms as described in the text.

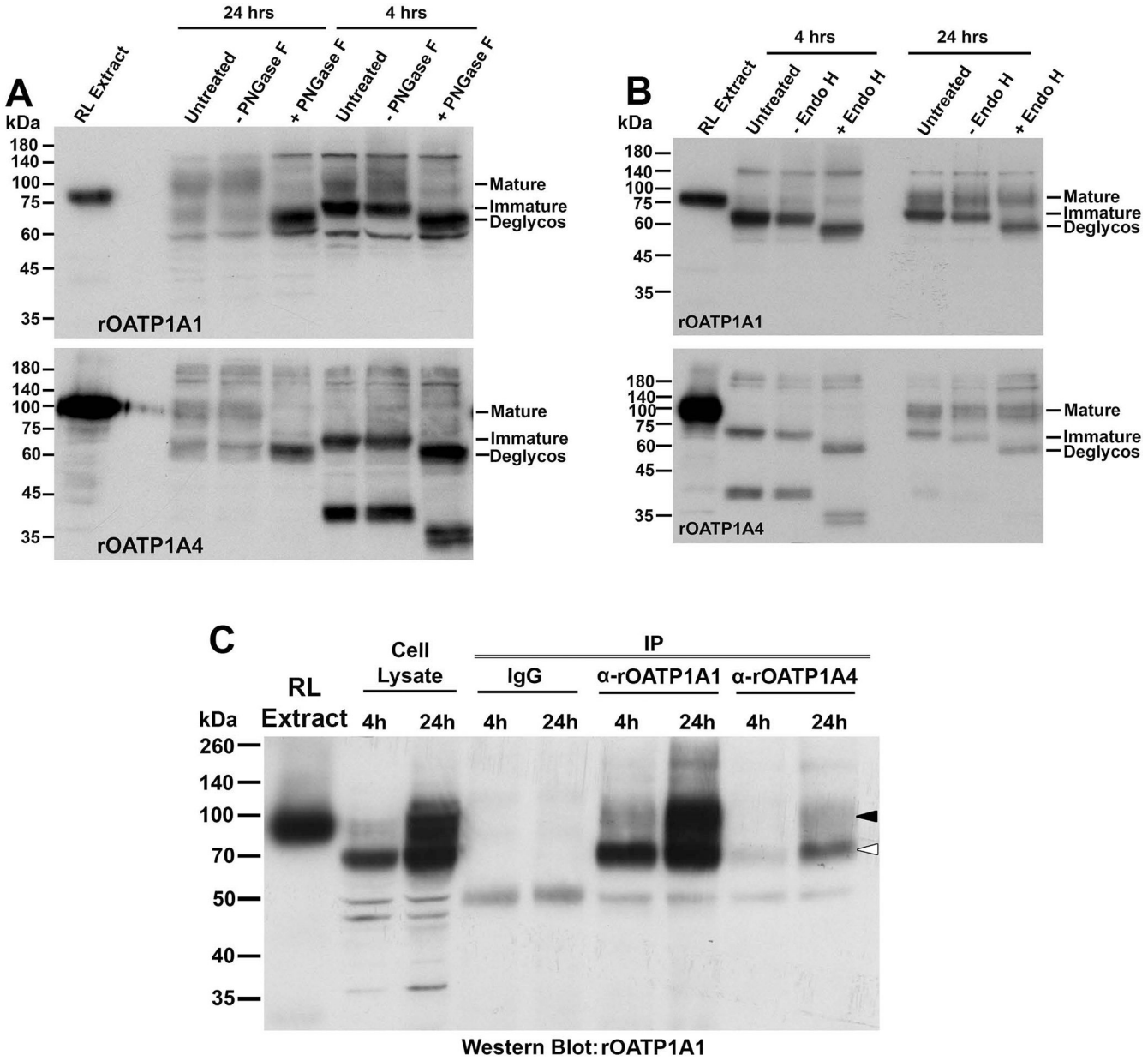

Figure 5: Assessment of the glycosylation state and interaction of rOATP1A1 and rOATP1A4 in stably transfected HeLa cells after induction of expression with zinc.

Panels A and B: HeLa cell lines expressing rOATP1A1 or rOATP1A4 under a metallothionein promoter were prepared and incubated for 4 or 24 hours, as indicated, in the presence of 150 μM zinc to initiate transporter expression. Cell lysates were prepared and were untreated or pretreated with buffer with or without PNGase F (panel A) or Endo H (panel B) prior to running immunoblots with antibody to rOATP1A1 or rOATP1A4 as indicated. A lane of rat liver homogenate that had been extracted with 0.1 M Na_2CO_3 (RL Extract) was included in each immunoblot to confirm antibody specificity. Positions of fully glycosylated, partially glycosylated, and fully deglycosylated OATPs are indicated on the right side of each immunoblot as mature, immature, and deglycos respectively. **Panel C:**

Cell lysates from doubly transfected HeLa cells incubated in zinc for 4 or 24 hours were subjected to immunoprecipitation with non-immune IgG or antibody against rOATP1A1 or rOATP1A4 as indicated and Western blot was performed to detect rOATP1A1.

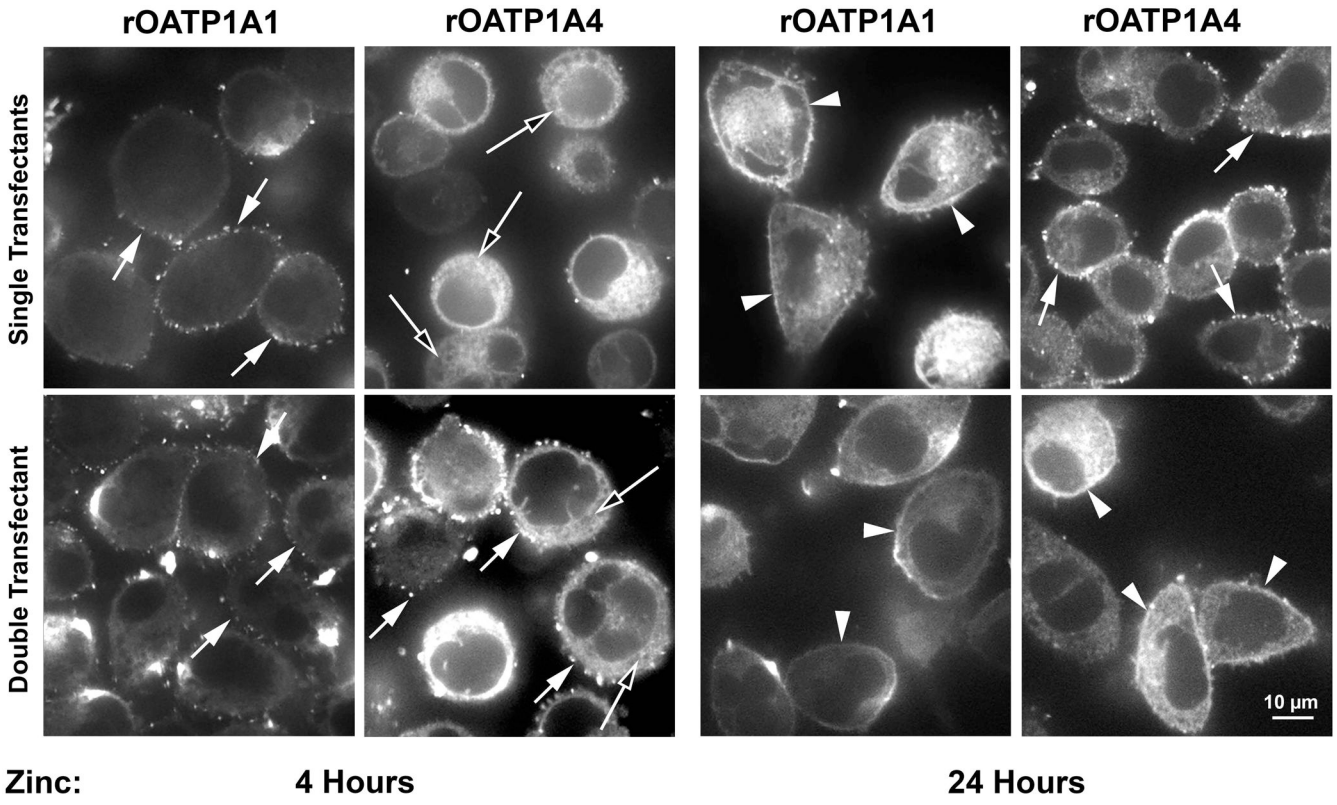

Figure 6: Expression of rOATP1A1 and rOATP1A4 in HeLa cells expressing each transporter individually and together.

Stably transfected HeLa cell lines expressing rOATP1A1, rOATP1A4, or both were incubated in zinc for 4 hours or 24 hours as described in Materials and Methods. Distribution of transporters was examined by immunofluorescence microscopy. Short arrows indicate punctate distribution of transporter on the cell surface. Long arrows indicate predominantly intracellular distribution. Arrowheads indicate smooth continuous surface distribution.

Table 1:

Saturation Kinetics of ^{35}S-BSP Uptake by HeLa Cells with Zn-dependent Expression of rOATP1A1 or both rOATP1A1 and rOATP1A4.

Cell Line	rOATP1A1			rOATP1A1 + rOATP1A4		
Time after Zinc	**0 hr**	**4 hr**	**24 hr**	**0 hr**	**4 hr**	**24 hr**
n	4	6	4	4	6	4
K_m	6.31 ± 3.83	1.88 ± 0.98	1.38 ± 0.73	6.14 ± 4.45	3.76 ± 1.83	1.52 ± 0.34
V_{max}	24.75 ± 12.57	24.0 ± 12.0	153.3 ± 44.4 *	34.3 ± 20.5	38.5 ± 25.0	97.6 ± 45.9 *
a	0.66 ± 0.99	0.68 ± 0.72	3.1 e-08 ± 8.5 e-09	1.00 ± 1.14	0.58 ± 0.53	0.19 ± 0.37

All cells were cultured for a total of 24 hours in the presence of 150 μM $ZnSO_4$ for 4 or 24 hr or in its absence as indicated. Uptake of ^{35}S-BSP was assayed at 24 hr as described in Methods.

* $p < 0.03$ as compared to cells at 0 or 4 hours after Zn addition.